

Cite this: *Chem. Sci.*, 2023, 14, 4401 All publication charges for this article have been paid for by the Royal Society of Chemistry

# Catalytic tandem dehydrochlorination–hydrogenation of PVC towards valorisation of chlorinated plastic waste†

Galahad O'Rourke,<sup>a</sup> Tess Hennebel,<sup>a</sup> Maxime Stalpaert,<sup>a</sup> Alina Skorynina,<sup>b</sup> Aram Bugaev,<sup>c</sup> Kwinten Janssens,<sup>a</sup> Lisa Van Emelen,<sup>a</sup> Vincent Lemmens,<sup>a</sup> Rodrigo De Oliveira Silva,<sup>a</sup> Christel Colemonts,<sup>d</sup> Philippe Gabriels,<sup>d</sup> Dimitrios Sakellariou<sup>a</sup> and Dirk De Vos<sup>a</sup>\*

Chemical treatment of end-of-life PVC at high temperature often results in the formation of polyacetylene and eventually aromatic char. These insoluble conjugated polymers lead to industrial reactor blockages, and limit the efficiency in recycling chlorinated plastic waste. To address this challenge, a solvent-based tandem dehydrochlorination–hydrogenation process is proposed for the conversion of PVC to a saturated polymer backbone. When combining tetrabutylphosphonium ionic liquids and homogeneous Rh catalysts under H<sub>2</sub> pressure, 81% dehydrochlorination is reached in 2 h, with the hydrogenation proceeding smoothly with minimal catalyst use of 0.5–2.0 mol% Rh. This process for PVC dechlorination yields soluble products that lack aromatics, have high degrees of dechlorination and possess a tunable content of double bonds. The chemical structures of the partially unsaturated polymer products and of the different structural motifs in the product are accurately monitored by a liquid <sup>1</sup>H-NMR method. Finally, X-ray absorption spectroscopy (XAS) sheds light on the catalytic Rh species during the tandem process, which are stabilized by the ionic liquid. This tandem process enables rapid PVC conversion to a saturated organic product, with polyethylene segments giving the opportunity for ensuing recycling steps.

Received 19th February 2023  
Accepted 30th March 2023

DOI: 10.1039/d3sc00945a

rsc.li/chemical-science

## Introduction

Plastic waste management is a pressing matter in contemporary consumer society. The end-of-life processing of polyvinyl chloride (PVC), polyvinylidene chloride (PVDC) and other chlorinated plastics remains challenging due to their high chloride content.<sup>1</sup> These chlorinated polymers, and especially PVC, which is the third most produced polymer worldwide, have many uses in construction, healthcare, electronics and the automotive sector with applications ranging from flooring to packaging material.<sup>2,3</sup> However, various additives with potential toxicity (e.g. phthalate plasticizers), or mixed plastic contaminants can impede mechanical recycling of PVC and limit the use of recyclates to low-end applications.<sup>4</sup> On the other hand, PVC valorization by thermal treatment is problematic, since beside

potential dioxin formation, PVC has a flame retardant effect that limits net energy recovery by incineration.<sup>5</sup>

Recent studies have considered ionic liquids as reaction media for thermal dehydrochlorination of PVC. Ionic liquids accelerate the dehydrochlorination by lowering the decomposition temperature, and act as solvents for PVC.<sup>6</sup> The cation and especially the anion of these ionic salts have been found to play a role in the dechlorination efficiency.<sup>7</sup> Additionally, phosphonium-based ionic liquids have shown promising results for the recycling of chlorinated multilayered blister packs.<sup>8</sup> In an effort to avoid landfilling or incineration, such chemical recycling by controlled thermal decomposition of PVC can allow the recovery of HCl that is eliminated from the chains. However, open literature procedures barely focus on the dechlorination products, which, due to their nature, would be difficult to process by industry. The main dehydrochlorination product, polyacetylene, is an extensively conjugated polymer which tends to crosslink to polyaromatic tar.<sup>7,9</sup> The insolubility of these products in practically all solvents leads to plugging of industrial reactors, thereby impeding further upcycling of the polymer carbon chain. If polyacetylene formation could be prevented, one could make PVC recycling more chemically feasible, with the potential of subsequent product transformations. Of the very few reports on such tandem transformations of PVC, a recent study demonstrated a tandem

<sup>a</sup>Centre for Membrane Separations, Adsorption, Catalysis and Spectroscopy for Sustainable Solutions (cMACS), KU Leuven, 3001 Leuven, Belgium. E-mail: dirk.devos@kuleuven.be

<sup>b</sup>ALBA Synchrotron, Cerdanyola del Valles, E-08290 Barcelona, Spain

<sup>c</sup>Paul Scherrer Institute, Forschungsstrasse 111, 5232, Villigen, Switzerland

<sup>d</sup>Vynova-group, 3980 Tessenderlo, Belgium

† Electronic supplementary information (ESI) available. See DOI: <https://doi.org/10.1039/d3sc00945a>



Fig. 1 Recycling of PVC. (top) Polyacetylenes, formed via pyrolysis and thermal degradation tend to crosslink to polyaromatic tar. (bottom) Solvent based tandem dehydrochlorination–hydrogenation, using ionic liquids and Rh catalysts, can lead to saturated polymers.

dechlorination–reduction–Friedel–Crafts alkylation.<sup>10</sup> While this divergent silylium catalysed process effectively converts PVC to polyethylene–polystyrene-like copolymers, it requires stoichiometric amounts of  $\text{Et}_3\text{SiH}$ , produces  $\text{Et}_3\text{SiCl}$  as a by-product and consumes part of the aromatic solvent for functionalization of the polymer backbone. So far, no atom efficient methods for PVC valorisation exist, that avoid simultaneous incorporation of carbon groups on the polymer backbone. In order to reduce the masses of the reactants needed, the dehydrochlorination is yet to be combined with maximally atom-efficient consecutive reactions.

Therefore, this investigation on PVC conversion looks beyond the formation of polyacetylene by simple dehydrochlorination and explores the possibility of a tandem dehydrochlorination–hydrogenation of PVC by the usage of  $\text{H}_2$ , as a potentially green reagent, and a homogeneous Rh hydrogenation catalyst. We hypothesize that in this combined catalytic reaction, the produced double bonds are hydrogenated, thereby ideally forming polyethylene type structures (Fig. 1). Minimal catalyst use, and avoiding stoichiometric reagents for dehydrochlorination such as silanes or metal hydrides, are important criteria on the road to a sustainable process that allows to tune the polymer product.<sup>10–12</sup>

## Results and discussion

### Solvent-based tandem dehydrochlorination–hydrogenation

Regarding the choice of the hydrogenation catalyst, we initially selected a homogeneous Rh(I) complex as the precatalyst, as prior investigations suggest activity of Rh for the hydrogenolysis of chlorobenzene derivatives and for hydrogenation of aromatics.<sup>13,14</sup> Initial reactions of PVC (1 mmol based on the molar mass of a monomer unit) in tetrabutylphosphonium chloride ( $\text{Bu}_4\text{PCL}$ , 3.5 eq.) with 2.0 mol%  $\text{H}(\text{CO})\text{Rh}(\text{PPh}_3)_3$  and  $\text{H}_2$ -pressure (20 bar) at 180 °C for 40 min, yielded a black

reaction mixture (Fig. 2). This mixture was washed with water–ethanol, to remove the excess of ionic liquid solvent, whereafter a black powder was obtained. It was found that this product was insoluble in known solvents for PVC (THF, butanone, cyclohexanone).<sup>15</sup> The color of this product and the limited solubility are caused by extensive cross-linking reactions which can occur with double bonds formed during the dehydrochlorination. Hence, the hydrogenation does not seem to work adequately when performed in pure ionic liquid, suggesting that the  $\text{H}_2$  has a too limited solubility in  $\text{Bu}_4\text{PCL}$ .<sup>16,17</sup> Instead of using pure ionic liquid, the reactions were therefore performed with the same reagents, but with the addition of a good solvent for  $\text{H}_2$  and PVC. This gave a significant difference in product outcome. After 40 minutes reaction in 2-butanone, at 180 °C and with 3.5 eq.  $\text{Bu}_4\text{PCL}$ , a precipitated yellow product was obtained (Fig. 2, 2A), while reactions in THF (Fig. 2, 2B) and cyclohexanone (Fig. 2, 2C) yielded again black products. The precipitation of the polymers occurred spontaneously during reaction, without the need for an antisolvent. Additionally, by  $^1\text{H}$  NMR no residual dissolved PVC was found in the solvent layer, indicating complete precipitation of the polymer product. Quantification by acid–base titration (see Experimental) showed that for each reaction after 40 min,  $41 \pm 5\%$  of the chlorine content of the PVC was released as HCl.

When applying the same reactions conditions, but limiting the amount of  $\text{Bu}_4\text{PCL}$  to only 0.85 eq. and using butanone as the solvent, no spontaneous product precipitation was observed after 40 min of reaction (Fig. 2, 3A). Hence it was necessary to recover the product by non-solvent addition (ethanol–water or a mixture thereof), and centrifugation to obtain the solid product in the form of a gel (Fig. 2, 3B). The mass of the recovered product was 51% of the initial mass of PVC. Titration on the other hand, showed that 60% of HCl was released in this reaction using a limited amount of ionic liquid. This indicates that a higher degree of dechlorination can be obtained when the





Fig. 2 (top) Pictures of reaction mixtures before and after the reactions: (1) PVC with only 3.5 eq. Bu<sub>4</sub>PbCl, without and with 2 mol% H(CO)Rh(PPh<sub>3</sub>)<sub>3</sub>-catalyst (1A and 1B, respectively); (2) PVC with 3.5 eq. Bu<sub>4</sub>PbCl and 2 mol% H(CO)Rh(PPh<sub>3</sub>)<sub>3</sub> in butanone (2A), THF (2B), cyclohexanone (2C); (3) PVC product with 0.85 eq. Bu<sub>4</sub>PbCl and 2 mol% H(CO)Rh(PPh<sub>3</sub>)<sub>3</sub> in butanone solvent (3A) and after product isolation (3B). (bottom) Three scenarios: case I: reaction in pure ionic liquid only leads to dehydrochlorination; case II: using an excess of ionic liquid in a solvent, the polymer precipitates spontaneously during reaction; case III: using a limited amount of ionic liquid in a solvent, spontaneous precipitation is avoided and largely saturated products are obtained.

product remains dissolved during the entire tandem process, than when spontaneous precipitation occurs during the tandem reaction. ATR FTIR on the purified polymer products

demonstrated a qualitative difference between PVC (Fig. 3A), the black products obtained after reaction in cyclohexanone with 3.5 eq. Bu<sub>4</sub>PbCl (Fig. 3B), and the yellow products, as



Fig. 3 ATR FTIR spectra and assignments of vibrational peaks. (A) PVC before reaction; (B) black precipitate formed after reaction with insufficient hydrogenation: significant C=O stretching and C=C bending peaks and char formation, indicated by a non-zero baseline (product obtained using 3.5 eq. of Bu<sub>4</sub>PbCl, 2 mol% H(CO)Rh(PPh<sub>3</sub>)<sub>3</sub>, in cyclohexanone at 180 °C for 2 h); (C) yellow product from effective tandem dehydrochlorination-hydrogenation, with intense C-H stretching vibrations and weakened C-Cl stretching vibrations (product obtained using 0.85 eq. of Bu<sub>4</sub>PbCl, butanone and 2 mol% H(CO)Rh(PPh<sub>3</sub>)<sub>3</sub> at 180 °C).

obtained in butanone (with 3.5 eq. or 0.85 eq.  $\text{Bu}_4\text{PbCl}$ ; Fig. 3C). The black products had a non-zero baseline, indicating char formation due to the absorption across the entire spectrum by carbon black. Beside this, double bonds were identified based on the  $\text{C}=\text{C}$  bending vibration ( $1077\text{ cm}^{-1}$ ). When exposed to air, the double bonds can easily get oxidized, leading to the detection of  $\text{C}=\text{O}$  and  $\text{C}-\text{O}$  vibrational peaks in the insufficiently hydrogenated product; this is consistent with literature relating to thermal degradation of PVC.<sup>18</sup> The FTIR spectrum of the yellow product (Fig. 3C) demonstrated effective tandem dehydrochlorination–hydrogenation, as evidenced by the intensity increase of the  $\text{C}-\text{H}$  vibrational peaks at  $2913\text{ cm}^{-1}$  ( $\nu_{\text{as}}\text{CH}_2$ ) and  $2846\text{ cm}^{-1}$  ( $\nu_{\text{s}}\text{CH}_2$ ), and a weakening of the  $\text{C}-\text{Cl}$  stretching ( $690\text{ cm}^{-1}$ ) and specific  $\text{C}-\text{H}$  bending vibration, which is associated to the presence of chloride ( $\delta\text{ CHCl}$ ,  $1250\text{ cm}^{-1}$ ).

Hence, while the IL is useful as a dehydrochlorination promoter, its use in excessive amounts seems unfavourable for the tandem dehydrochlorination–hydrogenation of PVC. Fig. 2 illustrates the three possible scenarios. Using pure ionic liquid (case I) leads to extensive dehydrochlorination but impedes hydrogenation, resulting in black char. When combining a large amount of IL with a solvent (case II), the hydrogenation is enhanced, but depending on the employed solvent, the product may still precipitate during the reaction and thus become inaccessible to the homogeneous Rh catalyst. In the ideal approach, the polymer remains entirely dissolved during dehydrochlorination thereby allowing an efficient consecutive hydrogenation in solution (case III). When using water as the non-solvent for product precipitation, one can easily determine the HCl yield in the water layer by titration, as a measure for the degree of dechlorination of PVC. When monitoring this reaction with 2 mol%  $\text{H}(\text{CO})\text{Rh}(\text{PPh}_3)_3$ , 0.85 eq.  $\text{Bu}_4\text{PbCl}$  and 1 mmol of PVC over the course of 2 h (Fig. 4), it can be seen that the

dehydrochlorination extent increases rapidly during the first hour when the ionic liquid is used. In opposition, a control reaction (without  $\text{Bu}_4\text{PbCl}$ , but with 2 mol%  $\text{H}(\text{CO})\text{Rh}(\text{PPh}_3)_3$  and heating of PVC at  $180\text{ }^\circ\text{C}$  in butanone), did not yield any HCl.

### Structure of polymer product

To give more solid proof for the reactions occurring during the proposed tandem dehydrochlorination–hydrogenation, solid state and liquid NMR were performed on the polymer products obtained using 0.85 eq.  $\text{Bu}_4\text{PbCl}$  and 20 bar  $\text{H}_2$  in butanone. While 2 mol%  $\text{HCO}(\text{Rh})(\text{PPh}_3)_3$  safely leads to a non-charred product, a Rh-catalyst loading of 0.5 mol% was found to be the minimum required to get a soluble product under these conditions. Lower catalyst loadings led to the black products as discussed before. A polymer product obtained after 2 h with this lowest catalyst loading was chosen for analysis by  $^{13}\text{C}$ -NMR, since it offers the best opportunity to observe intermediates. Firstly, the solid state spectrum of PVC (Fig. 5A) is marked by a loss of the tacticity information of the original polymer triad structure (VC-VC triads with VC representing vinyl chloride diads) due to peak broadening; the  $\text{CHCl}$  and  $\text{CH}_2$  groups have distinct broad peaks at 58 and 47 ppm, respectively. By liquid  $^{13}\text{C}$  NMR in  $d^8$ -THF (Fig. 5B) it can be observed that these two broad peaks are in fact composed of several signals representing the atactic composition of PVC. The atactic triad structure of PVC, which contains racemo (r) and meso diads (m), is reflected in three distinct peak groups in liquid  $^{13}\text{C}$ -NMR, both for the  $-\text{CHCl}-$  signals (55–58 ppm) and the  $-\text{CH}_2-$  signals (44–47 ppm). Secondly, the solid state NMR spectrum of the product (Fig. 5C) displayed a larger number of better resolved peaks than the PVC starting material using the same technique, which is indicative of a higher mobility of the polymer chains of the product.

The solid state MAS  $^{13}\text{C}$  spectrum of the dehydrochlorination–hydrogenation product is drastically different from that of the starting PVC, with the peaks of aliphatic hydrocarbon moieties now dominating the spectrum. Some peaks of residual  $-\text{CH}(\text{Cl})-$  appear in the  $\delta = 57\text{--}64\text{ ppm}$  region, which is the expected shift range for secondary alkyl chlorides. The weak signals at 46–47 ppm are as well reminiscent of the  $-\text{CH}_2-$  signals in the starting PVC. The very weak signal at 67 ppm may well arise from a small amount of tertiary chlorides. New signals appear in the  $\delta = 125\text{--}135\text{ ppm}$  region. Based on liquid  $^{13}\text{C}$  NMR (Fig. 5D), a clear correlation was found with  $^1\text{H}$  signals between 5.39 and 5.50 ppm in the HSQC-DEPT135 spectrum of the dissolved product (Fig. S4†). Therefore, these signals at 125–135 ppm can be unambiguously assigned to olefinic double bonds that were formed by dehydrochlorination, and which were not hydrogenated by the Rh catalyst. Additionally, no correlations with aromatic protons were found by HSQC, indicating that the product did not contain aromatic groups. The intense  $^{13}\text{C}$  peak at 29 ppm indicates that sequences of  $-\text{CH}_2-$  groups are now dominant in the polymer backbone, but the observation of a range of other signals (25–42 ppm) indicates that the structure does not resemble much that of pure polyethylene.<sup>19</sup> The peaks around 39 ppm could be ascribed either to (i)  $-\text{CH}_2-$  groups adjacent to isolated secondary  $-\text{CHCl}-$  units,

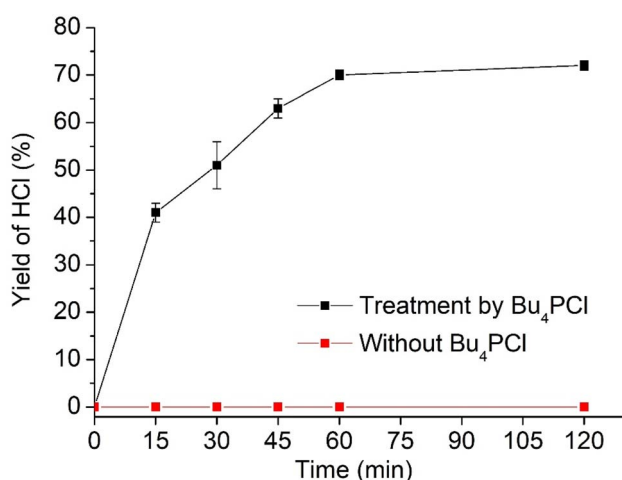


Fig. 4 Yield of HCl, determined by acid–base titration, during reaction of PVC with 0.85 eq.  $\text{Bu}_4\text{PbCl}$ , 2 mol% Rh at  $180\text{ }^\circ\text{C}$  in butanone, with rapid dehydrochlorination during the initial 60 minutes. Error bars represent the standard deviation. Control reaction of PVC without  $\text{Bu}_4\text{PbCl}$  in butanone yielded no HCl (conditions: 1 mmol PVC,  $180\text{ }^\circ\text{C}$ , 20 bar  $\text{H}_2$ , with 2 mol%  $\text{H}(\text{CO})\text{Rh}(\text{PPh}_3)_3$ ).



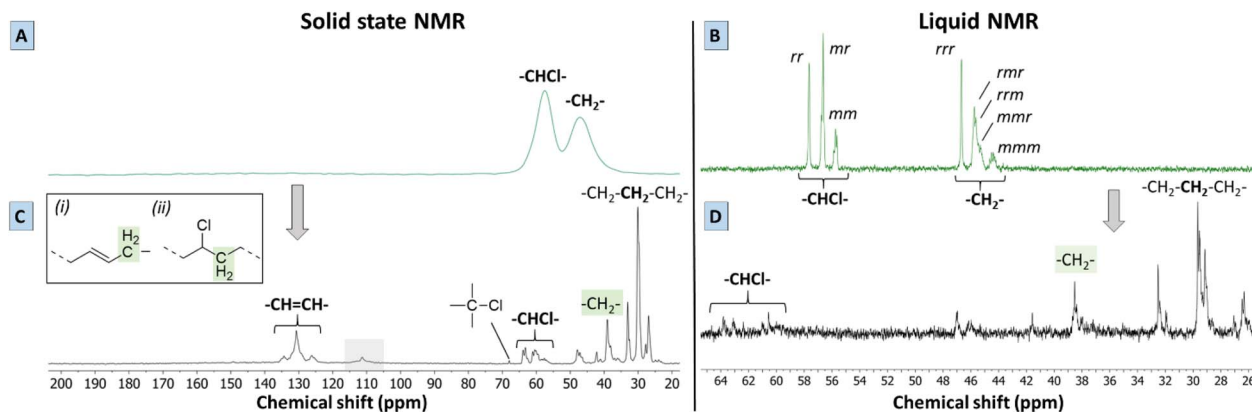


Fig. 5 Solid state (MAS) NMR spectra of PVC (A) and of the product (C) containing double bonds (130 ppm). In C, the signal at 110 ppm (grey box) is background signal from probe. Marked  $-\text{CH}_2-$  peaks comprise (i) allylic  $\text{CH}_2$ , (ii)  $\alpha$ - $\text{CH}_2$  next to  $-\text{CHCl}-$  groups. Liquid  $^{13}\text{C}$  NMR ( $\text{d}^8$ -THF, 400 MHz) shows tacticity of PVC (B) and microstructure of polymer product (D). The product has 81% dechlorination and 7 double bonds per 100 C from tandem dehydrochlorination–hydrogenation (0.5 mol%  $\text{H}(\text{CO})\text{Rh}(\text{PPh}_3)_3$ , 0.85 mmol  $\text{Bu}_4\text{PbCl}$ , 1 mL 2-butanone per 1 mmol PVC, 20 bar  $\text{H}_2$  at 180 °C).

or to (ii) allylic  $-\text{CH}_2-$  groups, in  $\alpha$  of newly formed  $\text{C}=\text{C}$  bonds. Finally, while the strong  $-\text{CH}_2-$  signals at  $\sim 27$  and  $\sim 33$  ppm are clearly of an aliphatic nature, they do not belong to a simple polyethylene chain. Candidate structures are (substituted) cyclohexyl rings, as well as  $-\text{CH}_2-$  groups adjacent to a tertiary  $-\text{CH}-$  branching point. The latter are more difficult to observe due to their lower abundance, and especially on cyclohexyl rings, tertiary signals can have variable shifts. The mechanisms leading to such structures will be discussed below. It is however clear that these rings or branched structures occur much more frequently than any of the known defects in the native PVC, where defects, such as methyl branches, affect typically  $\leq 1.5\%$  of the carbon atoms in the chain.<sup>12,20,21</sup> Thus, the branched or cyclic motifs observed in the reaction product must stem from the reaction itself, rather than from the original PVC backbone. Summarizing, the tandem PVC dehydrochlorination–hydrogenation in the ionic liquid leads to a highly saturated but non-linear polymer structure. Finally, it is to be remarked that the NMR spectra of the polymer product do not show any of the characteristic peaks of the  $\text{Bu}_4\text{PbCl}$  ionic liquid, proving that the IL is readily and fully removed.

Besides the detailed study of the  $^{13}\text{C}$  spectrum of the polymer product, its liquid  $^1\text{H}$ -NMR spectrum was used to quantify the degree of dechlorination of the product. The analysis, as elaborated in Section 4 of the ESI,<sup>†</sup> is based on integration of the signals of various  $\text{CHCl}$  groups and  $\text{CH}_2$  groups, in order to determine their relative abundance. In general, the products contain vinylic groups ( $-\text{CH}=\text{}$ ;  $\delta$  5.3–5.6 ppm), representing the formed double bonds;  $-\text{CHCl}-$  groups, adjacent to  $-\text{CH}_2-\text{CHCl}-$  segments, as subsisting from the initial VC–VC structure ( $\delta$  4.10–4.65 ppm); and isolated  $-\text{CHCl}-$  that is adjacent to ethylene units (E–VC–E, shift at 3.9 ppm); the latter are formed after partial dehydrochlorination with subsequent hydrogenation. Peaks of  $\text{CHCl}$  (VC–VC type), and  $\text{CHCl}$  (E–VC–E) contribute to the total fraction of chloride in the products and these peaks were found to correlate perfectly in HSQC with the  $^{13}\text{C}$  peaks at 58–64 ppm (Fig. S4<sup>†</sup>). Additionally, one observes

$\text{CH}_2-$  groups either in the  $\alpha$ -position to  $\text{CHCl}$  groups (VC units at  $\delta$  2.4–2.0 ppm), as in the original PVC structure, allylic protons ( $\delta$  2.0 ppm) and  $\text{CH}_2$ -groups ( $\delta$  1.28 ppm) in completely hydrogenated segments of the polymer product backbone, which are in so-called ethylene–ethylene (E–E) structures. This analysis allows quantification of all types of groups on the product and thus allows to determine the degree of dechlorination. By this method, the same polymer product that was investigated by  $^{13}\text{C}$ -NMR (Fig. 5) specifically showed a degree of dechlorination of 81%, and 7 double bonds per 100 carbon atoms. The  $^1\text{H}$ -spectra of products at various stages of dehydrochlorination–hydrogenation (obtained after variable reaction times with 1 mol% Rh) are shown in Fig. 6. More extensive reaction leads to a larger  $\text{CH}_2:\text{CHCl}$  ratio and thus higher degrees of dechlorination (Experimental, ESI Section 4<sup>†</sup>).

### Optimisation of reaction conditions

A search for the optimal conditions for the tandem reaction of PVC was performed with 0.85 mmol of  $\text{Bu}_4\text{PbCl}$  as the reaction promotor and  $\text{H}(\text{CO})\text{Rh}(\text{PPh}_3)_3$  as the hydrogenation catalyst, focusing on the degree of dechlorination of the polymer backbone as determined by  $^1\text{H}$ -NMR as the relevant optimization parameter. Firstly, variation of the temperature (Fig. 7A) showed that the reaction is fastest at 180 °C, with the dechlorination degree gently increasing up to 75% after 2 h of reaction. When comparing this curve with the HCl yield, as determined by titration (Fig. 4), the trends are very similar. Such data indicate that large amounts of HCl are available during the later phase of the reaction, and this will influence the structural changes of the eventual polymer product. Additionally, the NMR method allows quantification of each type of group on the polymer backbone. When following the tandem reaction with 2 mol% of  $\text{H}(\text{CO})\text{Rh}(\text{PPh}_3)_3$  catalyst at 180 °C (Fig. 7B), it is seen that after a 2 h reaction, only one double bond remains in the product; parallelly, the composition of the polymer backbone evolves from 50 to 88%  $\text{CH}_2$  groups. Additionally, in the first 15 minutes

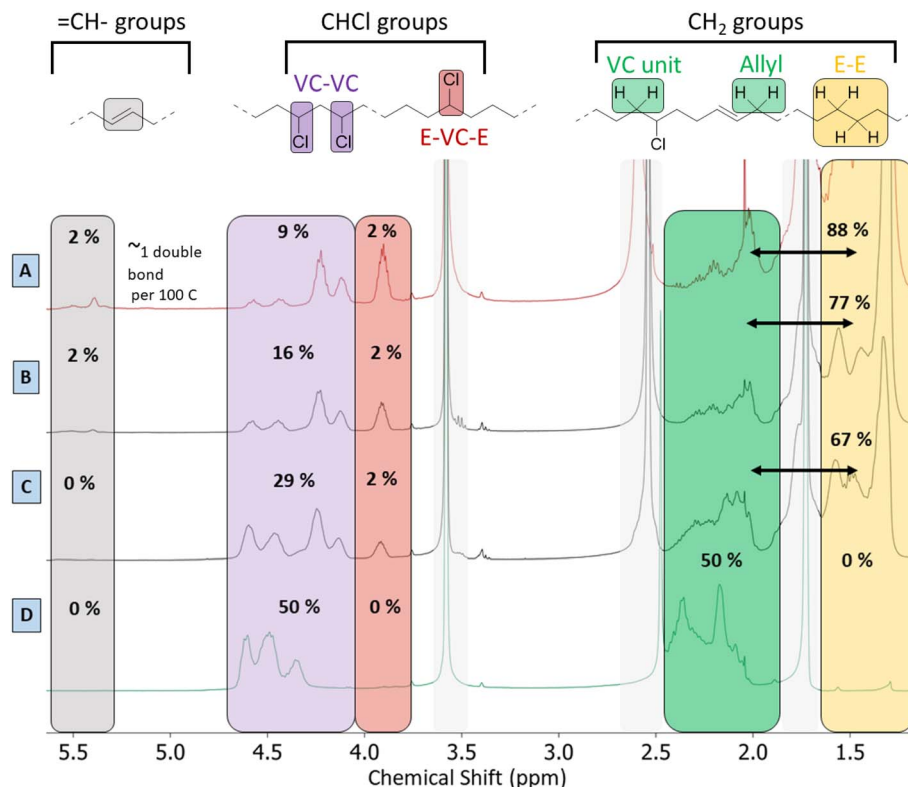


Fig. 6  $^1\text{H}$ -NMR spectra ( $\text{d}^8$ -THF, 400 MHz) of the tandem dehydrochlorination–hydrogenation products in various stages of dechlorination. Grey boxes indicate residual THF ( $\delta$  3.58, 1.71 ppm) and water ( $\delta$  2.51 ppm) peaks. The indicated percentages represent the determined carbon type fractions in each spectrum. PVC (62 mg, 1 mmol) was reacted with 0.85 mmol  $\text{Bu}_4\text{PbCl}$ , 1.0 mol%  $\text{H}(\text{CO})\text{Rh}(\text{PPh}_3)_3$  in 2-butanone at 180  $^\circ\text{C}$ , 20 bar  $\text{H}_2$ . With products obtained after (A) 2 h (with 78% dechlorination), (B) 45 min (with 64% dechlorination), (C) 15 min (with 38% dechlorination) and (D) virgin PVC (with 0% dechlorination).

of the reaction, isolated  $\text{CHCl}$ – groups, as part of ethylene–vinyl chloride–ethylene sequences ( $\text{E-VC-E}$ ;  $-(\text{CH}_2\text{CH}_2)-(\text{CH}_2-\text{CHCl})-(\text{CH}_2\text{CH}_2)-$ ) appear in the  $^1\text{H}$  NMR spectrum at 3.9 ppm; these  $-\text{CHCl}-$  groups represent a small fraction of 2% of the total number of carbon atoms. This fraction remained constant during the entire reaction, while the fraction of other  $\text{CHCl}$  groups, typically in  $\text{VC-VC}$  arrangements (4.1–4.6 ppm), decreases from 50 to 13%. This asserts that  $-\text{CHCl}-$  groups next to  $-(\text{CH}_2\text{CHCl})-$  units are dechlorinated faster, while the isolated  $-\text{CHCl}-$  groups (e.g. in  $\text{E-VC-E}$  arrangements) react much more slowly. Varying the Rh-catalyst loading between 2 and 0.5 mol% strongly influences the number of double bonds in the polymer backbone. When reducing the catalyst loading down to 0.5 mol%  $\text{H}(\text{CO})\text{Rh}(\text{PPh}_3)_3$ , up to 7 double bonds remain per 100 C atoms. Additionally, this reduced catalyst loading results in an enhanced dechlorination degree of the product of 81% (Fig. 7C and D). Further lowering of the catalyst loading resulted in product insolubility, suggesting that a too large number of (conjugated) double bonds increases the likelihood of cross-linking in the presence of released HCl.

Lowering the  $\text{H}_2$  pressure (from 15 to 5 bar  $\text{H}_2$ ) gave a similar effect as applying a low Rh catalyst loading. These findings suggest that the initial dehydrochlorination is sufficiently fast, and that the ensuing hydrogenation proceeds readily if enough catalyst and hydrogen are available. The fact that the eventual

degree of dechlorination is higher at lower Rh loading indicates that internal allylic chlorides on the polymer backbone play a significant role in the dehydrochlorination. Previous reports suggest a zipper-like mechanism for dehydrochlorination, in which initially formed allylic chloride moieties act as preferred sites for a quickly propagating dehydrochlorination.<sup>7,22</sup> When the rate of hydrogenation is too high, these allylic chlorides are hydrogenated to a less reactive  $-\text{CHCl}-$  in a saturated environment. Therefore, the rates of dehydrochlorination and hydrogenation must be matched to each other to achieve sufficient dechlorination degrees while avoiding char formation. Under the optimised conditions, with 0.5 mol% of Rh-catalyst, 81% of dechlorination was realized. Further increasing the reaction time under identical conditions to 26 h, gave only a 5% increase, to 86% dechlorination. In contrast to the non-hydrogenated dehydrochlorination products, which appear as black and brittle materials, the products of tandem dehydrochlorination–hydrogenation were yellow-whitish with an elastomeric appearance as a gel. Other catalyst precursors than  $\text{H}(\text{CO})\text{RhPPh}_3$  were also considered; it was found that 0.5–2 mol% of  $\text{RhCl}_3 \cdot \text{H}_2\text{O}$  displays the same hydrogenation activity in the tandem reaction of PVC with 0.85 mmol of  $\text{Bu}_4\text{PbCl}$  as  $\text{H}(\text{CO})\text{Rh}(\text{PPh}_3)_3$  (ESI, Fig. S7†).



Fig. 7 Dechlorination of PVC by tandem dehydrochlorination–hydrogenation (1 mmol PVC based on monomer, 0.85 mmol  $\text{Bu}_4\text{PCl}$ ). (A) Temperature influence on the extent of dechlorination using 2 mol%  $\text{H}(\text{CO})\text{Rh}(\text{PPh}_3)_3$ . (B) Fractions of groups in backbone of polymer product during reaction at 180 °C using 2 mol%  $\text{H}(\text{CO})\text{Rh}(\text{PPh}_3)_3$ . (C and D) Influence of  $\text{H}(\text{CO})\text{Rh}(\text{PPh}_3)_3$  loading on the degree of dechlorination and on the number of residual double bonds per 100 carbon atoms in the polymer product, at 180 °C. Quantification of products by liquid  $^1\text{H}$ -NMR ( $d^8$ -THF, 400 MHz).

### Mechanism of tandem dehydrochlorination–hydrogenation

Based on the  $^{13}\text{C}$ -NMR results, the  $^1\text{H}$ -NMR observations regarding the degree of dechlorination, and on the amounts of HCl released, as determined by acid–base titrations, a vision on the mechanism of the tandem dehydrochlorination–hydrogenation of PVC can be proposed. In the presence of an ionic liquid, PVC dehydrochlorination is generally considered to start by an ionic mechanism, rather than *via* radicals.<sup>7,23</sup> By analogy with the  $\text{Bu}_4\text{PCl}$ -mediated dehydrochlorination of 1,2-dichloroethane, an E2 mechanism is likely, with the chloride in non-aqueous media acting as a base accepting the proton. The acidity of the hydrogen atoms in PVC is also enhanced by the electron-withdrawing properties of the  $\text{Cl}^-$  substituents on the rest of the chain, which raise the susceptibility of  $-(\text{CH}_2\text{CHCl})-$  groups to E2 reactions. The E2 reaction initially leads to allylic chlorides, which react even faster since the formation of increasingly conjugated double bonds is a strong driving force for the elimination. Conversely, isolated  $-\text{CHCl}-$  groups in saturated parts of the chain are significantly less reactive. Thus, the overall dehydrochlorination is favored by maintaining a sufficient degree of unsaturation on the chains, *e.g.* by working with relatively low catalyst concentrations or hydrogen pressures. However, the availability of increasing amounts of

HCl and (conjugated) double bonds also raises the likelihood of carbocation formation on the chain (Fig. 8). An isolated secondary carbocation in a hydrocarbon chain could be expected to undergo isomerization, *e.g.* to form a methyl branch *via* a protonated cyclopropane intermediate. However, the NMR data ( $^{13}\text{C}$ ,  $^1\text{H}$ ) do not evidence any significant presence of methyl groups in the product. Therefore, reaction of the carbocation with a  $\text{C}=\text{C}$  bond, either in the same chain or on a different chain is much more likely. Intramolecular reaction could lead to cyclic structures, which after hydrogenation appear as saturated cycloalkyl groups. Intermolecular reaction leads to two chains being linked *via* a bond between two tertiary centers ( $\text{HR}_2\text{C}-\text{CHR}_2$ ). The  $^{13}\text{C}$  NMR data are consistent with both intra- and intermolecular routes.

To give a qualitative proof for the role of HCl in promoting intermolecular reactions between polymer chains, a tandem dehydrochlorination–hydrogenation reaction was performed with 0.85 eq.  $\text{Bu}_4\text{PCl}$ , 2 mol%  $\text{H}(\text{CO})\text{Rh}(\text{PPh}_3)_3$  in butanone and with 2 mmol HCl added in a concentrated dioxane solution from the start on. By  $^1\text{H}$ -NMR, the product after 30 minutes of reaction showed only 17% dechlorination, *versus* 50% in the absence of added HCl. This suggests that the dehydrochlorination could be to some extent reversible, especially since in our





Fig. 8 Mechanism of dehydrochlorination–hydrogenation of PVC: (A) dehydrohalogenation is faster for allylic chlorides than for isolated chlorides in a saturated chain; (B) intramolecular cyclization in a chain with several unsaturated bonds; (C) intermolecular reaction leading to cross-linking.

conditions, the HCl is not quenched, *e.g.* by addition of a strong base. More importantly, when HCl was added initially, a black insoluble product was obtained after 1 h of reaction, while in the reference reaction without added HCl, the product remained soluble even after 2 h of reaction, and reached a high degree of saturation. Thus, the accumulation of HCl clearly plays a role in the formation of insoluble products when the hydrogenation activity is not sufficiently high.

### Role of the ionic liquid

Since the best performance in the tandem process was observed with only 0.85 equivalents Bu<sub>4</sub>Pf<sub>6</sub> in butanone (or 25 mol% with respect to PVC), the effects of the chemical structure and concentration of the ionic liquid were investigated in more detail. In previous work using ILs for PVC dehydrochlorination, large excesses of IL with respect to PVC were used. For instance, Zhao used 13 equivalents of 1-butyl-3-methylimidazolium chloride with respect to the PVC monomer;<sup>24</sup> in earlier work on the non-reductive dehalogenation of PVC, we used 4.3 equivalents of Bu<sub>4</sub>Pf<sub>6</sub>.<sup>7</sup> From previous reports, clear influence of the halide of the ionic liquid on the decomposition temperature of PVC was observed. When using various halide anions in the ionic liquids, soluble products were only obtained with Bu<sub>4</sub>Pf<sub>6</sub> and Bu<sub>4</sub>Pf<sub>4</sub>, while Bu<sub>4</sub>Pf<sub>3</sub> led to high product insolubility even with the lowest equivalents. Hence, in order to better understand these halide effects, model reactions were performed with 2-chloropentane as a reactant, in the same ionic liquids, at 140 °C for 2 h (Fig. 9A and C). When changing the anion of the IL, the chloropentane conversion increases in the order Cl<sup>−</sup> < Br<sup>−</sup> < I<sup>−</sup>. While elimination of HCl to form pentenes is the only reaction observed in Bu<sub>4</sub>Pf<sub>6</sub>, substitution reactions, with formation of 2-bromopentane or 2-iodopentane become

increasingly dominant in the same order Br<sup>−</sup> < I<sup>−</sup>. This obviously reflects an increasing nucleophilicity as the size and polarizability of the halide anion increase (Fig. 9C). As is apparent from the chloropentane conversion, the change of the halide from Cl<sup>−</sup> to Br<sup>−</sup> enhances the dechlorination degree of the product, with the Br-phosphonium salt performing better than its Cl-based counterpart. Changing the cation of the ionic liquid from Bu<sub>4</sub>Pf<sub>6</sub> to Ph<sub>4</sub>Pf<sub>6</sub> gave almost no reaction of the model compound; this again underscores the unique effect that tetraalkylphosphonium cations have on the properties of the halide ions, especially on their basicity and nucleophilicity.

In view of these results, the higher PVC dechlorination rates in Bu<sub>4</sub>Pf<sub>6</sub> and Bu<sub>4</sub>Pf<sub>4</sub> ionic liquids can be ascribed to nucleophilic substitutions on the PVC backbone, creating C–Br or C–I bonds. Because of the superior leaving group properties of bromide in comparison to chloride, the subsequent dehydrohalogenation proceeds more readily, causing acceleration of the entire dehalogenation process of PVC (Fig. 9A). In the Bu<sub>4</sub>Pf<sub>6</sub> ionic liquid, the PVC dehydrochlorination is so rapid that an insoluble product is formed even before sufficient saturation of the chains can occur. Hence, the analysis of the influence of different substoichiometric amounts of ionic liquids in the tandem dehydrochlorination–hydrogenation of PVC shows that no soluble products for quantification were obtained using Bu<sub>4</sub>Pf<sub>6</sub>, but using Bu<sub>4</sub>Pf<sub>4</sub> as the ionic liquid systematically resulted in higher dehydrochlorination rates than with Bu<sub>4</sub>Pf<sub>6</sub>, in all applied molar ratios (Fig. 9B) because of the additional occurrence of nucleophilic substitution reactions.

### Characterization of the homogeneous Rhodium catalyst

The solidification of the IL at room temperature ( $T_{\text{melting}} = 64^\circ\text{C}$ ) was used as a unique feature to trap the active catalytic







**Fig. 9** Role of the ionic liquid counter ion. (A) Conversion of 2-chloropentane in various ionic liquids at 140 °C (0.5 mmol chloropentane with 0.85 mmol ionic liquid); proposed reactions of PVC in Bu<sub>4</sub>PBr. (B) Variation of ionic liquid loading and type for tandem reaction of PVC (2.0 mol% H(CO)Rh(PPh<sub>3</sub>)<sub>3</sub>, variable equivalents of Br or Cl-based ionic liquid, 1 mL 2-butanone per 1 mmol PVC, 20 bar H<sub>2</sub> at 180 °C, 2 h). (C) Conversion of 2-chloropentane using various ionic liquids (determined by gas chromatography) by nucleophilic substitution and elimination, as promoted by ionic liquids.

species during the tandem dehydrochlorination–hydrogenation.<sup>25</sup> X-ray absorption spectroscopy (XAS) was performed at the European Synchrotron Radiation facility (ESRF, Grenoble) for the characterization of the Rh species at high energies (23.2 keV). To unravel the speciation of the catalyst, *ex situ* samples of Rh catalysts immobilized in IL were measured before and after reaction under optimal conditions (*vide supra*) and compared to reference spectra (ESI, Table S1†). The obtained X-ray absorption near edge structure (XANES) and the extended X-ray

absorption fine structure (EXAFS) spectra are reported in Fig. 10.

First, the H(CO)Rh(PPh<sub>3</sub>)<sub>3</sub> catalyst was characterized in both Bu<sub>4</sub>PCl and Bu<sub>4</sub>PBr, before and after reaction, to investigate structural changes in the Rh coordination sphere during reaction, with respect to the applied ionic liquid. Overall, the catalyst maintains a similar oxidation state before and after reaction (solid and dashed line), as no shift in the edge jump was observed in the XANES. However, in EXAFS there is a clear shift



Fig. 10 Left: XANES (a) and phase-uncorrected FT-EXAFS (b) data for the active Rh catalyst  $\text{H}(\text{CO})\text{Rh}(\text{PPh}_3)_3$  trapped in  $\text{Bu}_4\text{PCL}$  (blue) and  $\text{Bu}_4\text{PBr}$  (red); characterized before (solid line) and after reaction (dashed line) with PVC. Right: XANES (c) and phase-uncorrected FT-EXAFS (d) data for the Rh catalyst in  $\text{Bu}_4\text{PCL}$  (blue, solid and dashed, before and after reaction), and comparison to  $\text{RhCl}_3$  in  $\text{Bu}_4\text{PCL}$  after reaction with PVC (orange); reference compounds  $\text{RhCl}_3$  (green) and Rh-foil (gray). Detailed descriptions of the samples can be found in the ESI, Table S1.†

towards larger bond distances in the Rh coordination sphere. Presumably, this results from a loss of the lighter elements ( $\text{H}$ ,  $\text{CO}$ ,  $\text{PPh}_3$ ) in favor of significantly heavier halides ( $\text{Cl}^-$ ,  $\text{Br}^-$ ), as a consequence of the high halide content in the reaction medium.<sup>25</sup> The observed shift is more pronounced in the brominated  $\text{Bu}_4\text{PBr}$  IL, where after reaction one finds a high concentration of  $\text{Cl}^-$  originating from the high degree of PVC dechlorination, and of  $\text{Br}^-$  from the ionic liquid itself (*cf. supra*, *Role of the ionic liquid*). After reaction in  $\text{Bu}_4\text{PCL}$ , the final Rh catalyst shows similar features as obtained with  $\text{RhCl}_3$ . This provides additional proof of the ligand substitution with halides under the applied conditions. In order to confirm the true homogeneous nature of the Rh catalyst, a comparison was made with Rh foil. This indicated that the catalyst is ionic and monometallic, as no  $\text{Rh}^0$ , nor Rh–Rh contributions were observed in the experimental samples. Relating to catalyst stability, it could also be verified experimentally that the formed Rh–Cl species is stable in the ionic liquid during at least three reaction cycles (ESI, Section 7, Fig. S9 and S10†).

## Conclusion

Conversion of PVC by tandem catalytic dehydrochlorination–hydrogenation was proposed as a highly effective method to achieve high dechlorination degrees of PVC. As additional advantages, soluble products are obtained, and  $\text{H}_2$  is an efficient, waste-free reagent for the reduction. In contrast to other methods for PVC recycling which use reducing agents like silanes, or metal hydrides it was found the limited quantities of ionic liquid and Rh-catalyst can reach high conversion to PE-like structures. Additionally, the PVC does not have to be

pretreated by drying before reaction because dehydrochlorination–hydrogenation promoters are not as sensitive to moisture.<sup>10</sup> The double bond content of the product can be tuned by varying the concentration of the Rh hydrogenation catalyst. The active Rh species was found to be of ionic nature, and to occur predominantly as homogeneous Rh chloride complexes, which are formed in the ionic liquid medium during the PVC dehydrochlorination reaction. Mechanistically, the  $\text{HCl}$  elicits rearrangements on residual double bonds of the product, leading to saturated tertiary branching points or cycloaliphatic structures. The findings indicate that the ionic liquids play a critical role in facilitating the  $\text{HCl}$  elimination reactions.<sup>8</sup> Initial recyclability tests indicate that the applied Rh-catalysts are stable under the reaction conditions for three consecutive reaction cycles.

Further work will be directed towards functionalizing or selectively splitting the double bonds for enhanced PVC valorization after the tandem conversion process.<sup>26,27</sup> Additionally, the influence of different types of additives on the tandem process will be investigated for typical PVC waste applications.<sup>22,28–31</sup>

## Experimental

PVC powder ( $M_w \sim 43\,000$ ,  $M_n \sim 22\,000$ ),  $\text{Bu}_4\text{PCL}$  (96%),  $\text{Bu}_4\text{PBr}$  (98%) and  $\text{Bu}_4\text{PI}$  (98%) were supplied as solid powders by Sigma-Aldrich. 2-Butanone (technical grade, 99%), THF (>99.9%), and cyclohexanone (99%) solvents were acquired from the same supplier.  $\text{RhCl}_3 \cdot \text{H}_2\text{O}$  and  $\text{H}(\text{CO})\text{Rh}(\text{PPh}_3)_3$  were supplied by TCI. The reagents nor the PVC were additionally purified or dried before use.



## Tandem dehydrochlorination–hydrogenation reactions

The reactions were performed in homemade metal alloy autoclave reactors which can withstand pressures up to 60 bar. PVC (1 mmol based on the monomer unit with molar mass of 62.6 g mol<sup>−1</sup>, 62.5 mg), Bu<sub>4</sub>PfCl (0.85 mmol, 250 mg) and H(CO)Rh(PPh<sub>3</sub>)<sub>3</sub> (2 mol%, 18.4 mg) or varying quantities as described otherwise, were brought into a glass liner. Thereafter, the solvent (1 mL) was added to the glass liner, which was then placed inside the reactor. Subsequently, the reactor was sealed and purged twice with N<sub>2</sub>-gas before filling it with 20 bar of H<sub>2</sub>-gas. The reaction mixture was then stirred (750 rpm) at elevated temperature (100–180 °C). After heating for the designated time, the reaction was quenched by cooling the reactor in an ice bath. The solvent layer was decanted and the precipitated polymer was dissolved in THF for purification. Thereafter, the polymer was precipitated again by the dropwise addition of water to the solvent layer. After isolation of the precipitated polymer product, it was washed three times with water (2 mL) and ethanol (2 mL). Finally, the product was subjected to an air stream to remove excess solvent and dried at 60 °C under reduced pressure overnight. Optimisation reactions were done in triplicate. Curves show mean values ± standard deviation as error margin.

## HCl yield determination

The HCl yields in tandem PVC dehydrochlorination reactions were quantified by acid–base titration of the recovered solvent layer (1 mL). This layer was diluted with water (6 mL) and titrated with a 0.05 M KOH solution. A correction was taken into account for the acidity of the ionic liquid by titrating Bu<sub>4</sub>PfCl (0.85 mmol, 250 mg) diluted in water (6 mL). Experiments were done in triplicate.

## Determination of dechlorination degree by NMR

The dechlorinated polymer products (samples of ±5 mg) were dissolved at 50 °C in d<sup>8</sup>-THF. The obtained polymer solutions were measured by liquid <sup>1</sup>H-NMR at room temperature on a 400 MHz Bruker Avance III HD spectrometer. The dechlorination degree was determined by integrating the <sup>1</sup>H-NMR spectrum and calculating the relative fractions of each type of carbon in the polymer chain. Each integral area is divided by the number of protons per corresponding carbon group. The sum of all types of carbon groups is then equalled to 100%, and the fraction of each carbon type in the polymer backbone can be calculated. The degree of dechlorination is defined as: 100% – (number of residual CHCl in product)/(number of CHCl groups initially in PVC). An example is described in the ESI.†

## Influence of ionic liquids

2-Chloropentane conversion in the presence of ionic liquids was determined by gas chromatography (GC), using a Shimadzu GC-2010 device, with CP Sil-5 column. Quantification and calibration of the flame ionisation detector (FID) response were done by the effective carbon number (ECN) method (ECN (2-halopentane): 4.88, ECN (pentene): 4.9, ECN (pentane): 5).

Reactions were performed in autoclaves with a 2-chloropentane stock solution (0.5 mmol, 1.0 M, 1 mL) and the ionic liquid (0.85 mmol of Bu<sub>4</sub>PfCl, Bu<sub>4</sub>PfBr, Bu<sub>4</sub>PfI or Ph<sub>4</sub>PfCl) added to the glass liner. After stirring for 2 h at 140 °C under 20 bar H<sub>2</sub>, the autoclaves with reaction mixtures were cooled to 0 °C in an ice bath before GC analysis.

## XAS data collection and analysis

XAS measurements were performed in transmission mode by continuous scanning of a Si(311) double-crystal for Rh K-edge at the BM23 beamline of the ESRF (Grenoble, France). The RhCl<sub>3</sub> reference was pressed into a pellet to optimize the absorption jump at the Rh K-edge. The samples were sealed inside 5 mm Teflon rings of optimal thickness and covered with Kapton tape. For each sample, 10 spectra were collected and then averaged to improve signal-to-noise ratio. The energy sampling steps were 0.5 eV. The Rh foil was used as a reference sample and was installed between 2nd and 3rd ionization chambers. Experimental XAS data processing, including normalization, energy calibration, extraction of  $\chi(k)$  signals and further Fourier analysis of EXAFS, were performed in the Demeter package.<sup>32</sup>

## Data availability

Original data are available within KULeuven's OneDrive system. The ESI† contains additional characterisation data and conditions of experiments.

## Author contributions

O'Rourke G. wrote the original draft, did editing, conceptualization and conducted experimental work. Hennebel T., Stalpaert M., Van Emelen L., Lemmens L. measured samples related to XAS or conducted experiments. De Oliveira R. and Sakellariou D. enabled the solid state NMR methodology and performed measurements. Bugaev A. and Skorynina A. conducted XAS modelling. Janssens K. was involved in the communication and reporting of the XAS data. Colemonts C. and Gabriels P. gave advice in the investigation. De Vos D. supervised the investigation, edited the manuscript with conceptualization.

## Conflicts of interest

There are no conflicts to declare.

## Acknowledgements

This work was financially supported by Vynova and the authors thank Peter Van der Veken and Viviane Vandenberghe for their industrial expertise on the project. The authors are also grateful to Jannick Vercammen, Sam Van Minnebruggen and Simon Smolders for measuring the XAS samples. G. O., K. J., V. L., L. V. E. and D. D. V. thank FWO (G0F2320N) for financial support. We acknowledge the European Synchrotron Radiation Facility for providing the beamtime (proposal MA-4443 and MA4926) at



BM23 beamline and Dr Kirill Lomachenko for the professional support.

## References

- 1 T. Okada, S. Sutoh, K. Sejima, H. Tomohara and S. Mishima, *Polym. Degrad. Stab.*, 2020, **171**, 109040.
- 2 PlasticsEurope, *Plast. – Facts 2018*, 2018, p. 38.
- 3 J. Yu, L. Sun, C. Ma, Y. Qiao and H. Yao, *Waste Manag.*, 2016, **48**, 300–314.
- 4 S. Windels, T. Diefenhardt, N. Jain, C. Marquez, S. Bals, M. Schlummer and D. E. De Vos, *Green Chem.*, 2022, **24**, 754–766.
- 5 J. Hiltz, R. S. Underhill, H. Moyst, *Technical Report*, Defence R&D Canada – Atlantic, 2007.
- 6 T. Zhao, Q. Zhou, X. L. He, S. Di Wei, L. Wang, J. M. N. van Kasteren and Y. Z. Wang, *Green Chem.*, 2010, **12**, 1062–1065.
- 7 D. Glas, J. Hulsbosch, P. Dubois, K. Binnemans and D. E. Devos, *ChemSusChem*, 2014, **7**, 610–617.
- 8 K. Oster, A. Tedstone, A. J. Greer, N. Budgen, A. Garforth and C. Hardacre, *Green Chem.*, 2020, **22**, 5132–5142.
- 9 Y. J. Choi, J. H. Kim and J. S. Im, *J. Mater. Res. Technol.*, 2021, **14**, 2845–2852.
- 10 M. K. Assefa and M. E. Fieser, *J. Mater. Chem. A*, 2023, **11**, 2128–2132.
- 11 L. Monsigny, J. C. Berthet and T. Cantat, *ACS Sustain. Chem. Eng.*, 2018, **6**, 10481–10488.
- 12 W. H. Starnes, *J. Polym. Sci. Part A Polym. Chem.*, 2005, **43**, 2451–2467.
- 13 F. Alonso, I. P. Beletskaya and M. Yus, *Chem. Rev.*, 2002, **102**, 4009–4091.
- 14 C. Vangelis, A. Bouriazos, S. Sotiriou, M. Samorski, B. Gutsche and G. Papadogianakis, *J. Catal.*, 2010, **274**, 21–28.
- 15 G. Grause, S. Hirahashi, H. Toyoda, T. Kameda and T. Yoshioka, *J. Mater. Cycles Waste Manag.*, 2017, **19**, 612–622.
- 16 A. Kordi and F. Sabzi, *Int. J. Hydrogen Energy*, 2018, **43**, 18296–18305.
- 17 B. R. Mellein, A. M. Scurto and M. B. Shiflett, *Curr. Opin. Green Sustain. Chem.*, 2021, **28**, 100425.
- 18 R. R. Stromberg, S. Straus and B. G. Achhammer, *J. Res. Natl. Bur. Stand.*, 1958, **60**, 147.
- 19 Z. Zhou, C. Anklin, R. Kuemmerle, R. Cong, X. Qiu, J. Decesare, M. B. Kapur and R. Patel, *Macromolecules*, 2021, **54**, 5985–5990.
- 20 D. Braun, G. Holzer and T. Hjertberg, *Polym. Bull.*, 1981, **5**, 367–372.
- 21 W. H. Starnes, F. C. Schilling, I. M. Plitz, R. E. Cais and F. A. Bovey, *Polym. Bull.*, 1981, **4**, 555–562.
- 22 P. Zhao, T. Li, W. Yan and L. Yuan, *Environ. Technol.*, 2018, **39**, 977–985.
- 23 V. H. Tran, A. Guyot, T. P. Nguyen and P. Molinié, *Polym. Degrad. Stab.*, 1992, **37**, 209–216.
- 24 T. Zhao, Q. Zhou, X.-H. Jiang, A.-K. Du and Y.-Z. Wang, *5th ISFR*, 2009, pp. 260–262.
- 25 K. Janssens, A. L. Bugaev, E. G. Kozyr, V. Lemmens, A. A. Guda, O. A. Usoltsev, S. Smolders, A. V. Soldatov and D. E. De Vos, *Chem. Sci.*, 2022, **13**, 10251–10259.
- 26 P. Liu and C. Ai, *Ind. Eng. Chem. Res.*, 2018, **57**, 3807–3820.
- 27 A. Dewaele, T. Renders, B. Yu, F. Verpoort and B. F. Sels, *Catal. Sci. Technol.*, 2016, **6**, 7708–7717.
- 28 S. S. Suresh, S. Mohanty and S. K. Nayak, *J. Clean. Prod.*, 2017, **149**, 863–873.
- 29 M. Chantreux, D. Ricard, L. Asia, S. Rossignol and P. Wong-Wah-Chung, *Radiat. Phys. Chem.*, 2021, **188**, 109671.
- 30 J. Miliute-Plepiene, A. Frâne and A. M. Almasi, *Clean. Eng. Technol.*, 2021, **4**, 100246.
- 31 S. Kim, *Waste Manag.*, 2001, **21**, 609–616.
- 32 B. Ravel and M. Newville, *J. Synchrotron Radiat.*, 2005, **12**, 537–541.

